# Nonlinear Unsteady Motions and NOx Production in Gas Turbine Combustors

G. Swenson, W. Pun, and F. E. C. Culick

Jet Propulsion Center
California Institute of Technology, Pasadena, California, 91125 USA

**Abstract**

Chiefly for improved efficiency, the trend to increasing use of gas turbine engines in stationary powerplants has been firmly established. The requirement for minimum NOx production has motivated operation as close as practically possible near the lean flammability limit, to reduce flame temperatures and consequently reduce formation of nitrogen oxides via the Zeldovich thermal mechanism. However, experience has shown that under these conditions, stability of the chamber is compromised, often leading to the presence of sustained oscillations in the combustor. That possibility raises the problem of the influence of oscillatory motions on the production of nitrogen oxides. Numerically calculating these influences for a complex geometry gas turbine combustor is too computationally expensive at this time. Nonlinear analytical methods making use of these influences are a promising direction for simpler ways to design and develop operational gas turbine combustors. However, this analysis needs results on which to base unsteady models of the interaction between nonlinear oscillations and species production within a gas turbine combustor. In this paper, two methods are explored briefly as an initial step. The first is based on a configuration of perfectly stirred and plug flow reactors to approximate the flow in a combustion chamber. A complete representation of the chemical processes is accommodated, but the geometry is simplified. The second is a full numerical simulation for a realistic geometry, but at this stage the chemistry is simplified.

## Introduction

The rate of formation of unwanted chemical species depends on both detailed local chemical kinetics and on the various aspects of fluid mechanics comprising both local and global influences. Past experimental and numerical efforts have been largely concerned with the determination of steady state or time averaged values of these chemical species for a wide range of operating conditions. However, the flow field in a combustor is rarely steady, owing to the inevitable fluctuations associated with local instabilities, including regions of flow separation, and to the presence of substantial noise arising from a variety of sources. Hence, it is quite possibly more appropriate and practically useful to examine the formation of pollutants, in particular nitrogen oxides, under dynamic conditions. The work in this paper will set forth methods for the determination of various chemical species under dynamic conditions. Results of this work will eventually lead to analytical tools to describe the influence of flow field oscillations on chemical production rates. These analytical tools will be developed further in subsequent work.

Because combustors necessarily contain high densities of energy production, and possess relatively low losses for unsteady motions in the flow, the general problem of instabilities - generically called 'combustion instabilities' - has been encountered in all types of propulsion systems and stationary powerplants. Analyses have been carried out at various levels of complexity and with varying degrees of success. The approach taken here amounts to extension of the methods used with considerable success in analyzing combustion instabilities in rockets and ramjets [1-4]. The eventual purpose is to develop methods for predicting the formation of pollutants in the presence of organized oscillations and random motions or noise. In the present work, we are concerned with numerical methods directed to the eventual construction of local 'response functions' for unsteady formations of NOx and other chemical species.

Environmental concerns have led to increased restrictions on pollutant emissions of gas turbine combustion systems. The strict standards have increased the efforts by researchers to understand the mechanisms behind pollutant formation (NOx, CO, UHC) in order to reduce emission levels. One of the efforts in the reduction of emissions has been in the development of lean premixed combustion (LPC). Recent efforts to examine NOx formation in LPC have been reviewed by Correa [5]. The general strategy is to decrease the NOx level with a decrease in the equivalence ratio and a corresponding decrease in flame temperature which reduces the amount of NOx produced according to the Zeldovich thermal mechanism.

Another consequence of LPC is that combustion is pushed toward the lean flammability limit, which has been shown experimentally to have reduced stability and a greater chance of developing sustained oscillations.

Current computational and experimental works in the field of LPC [6-8] examine steady state or time averaged pollutant values at a set operating condition. The goals are scaling laws relating pollutant levels to pressure and temperature design conditions. Those relations apply to steady conditions; however, the predicted values may show variations within an oscillating flow field. The report by J. O. Keller and I. Hongo [9] provides some results for pollutant emissions in a pulse combustor under pulsing and non-pulsing conditions. Significantly higher NOx was produced in the main flame zone while significantly less NOx was expelled at the exit plane under pulsing conditions. The higher levels in the main flame zone are likely due to an exponential dependence of NOx levels on temperature, leading to an increase in the average NOx levels in the presence of an oscillating temperature field. The explanation given for the lower NOx output at the exit plane was based on the idea that the shorter residence time at high combustion temperatures reduced the impact of the Zeldovich thermal mechanism. In the non-pulsing case, the temperature remained high downstream of the flame, allowing more time for the completion of NOx production. However, in the pulsing case, the temperature field dropped off significantly after the peak flame temperature, reducing the residence time at high temperature and hence lowering the emission level. The interpretations given in that paper are largely speculative; neither sufficiently detailed experimental results nor any analysis exists to support the conclusions.

The development of analytical models is important for the design and evaluation of gas turbine combustors. The models should provide a means of describing how chemical species and thermodynamic fluctuations affect each other. The models should also make use of both local and global interactions within the flow field. For the models to be developed and for this interaction to be better understood, results, either experimental or numerical need to be obtained. This paper will describe numerical work currently in progress to meet these requirements. The first method makes use of a combination of PSRs (perfectly stirred reactors) and PFRs (plugged flow reactors) to compute the effects of oscillations with complete chemistry, but a simplified geometry. The second method is numerical modeling of the complex geometry of a gas turbine test combustor with simplified chemistry in an initial step to examine more

closely how the overall flow field might impact chemical production rates. Both of these methods are approximations to a complete simulation of reacting flow within a full scale detailed geometry and with a faithful representation of the actual chemistry.

This paper has two purposes: (1) to outline the application of an approximate analysis to the problem of determining the effects of coherent oscillations and noise on the formation of NOx; and (2) to give initial results for the influences of flow field oscillations on the level of various species including NOx and CO.

## Background: Formulation of an Approximate Analysis

It is presently not reasonable to attempt a complete analysis of a flow in a combustor to determine the production of pollutants, whether or not organized oscillations are present. The numerical methods of CFD might be adequate but the basis for applying them has not been fully developed and applications are computationally expensive. A comprehensive theory encompassing large scale non-uniform motions, small-scale turbulence, detailed finite-rate chemistry and interactions between turbulence and chemical kinetics is not available [5-10]. In any event, analytical work is necessarily approximate. Since our attention here is directed to the possible influences of oscillations in the flow on the rate at which pollutants are formed, it seems a rational strategy to investigate the possibility of extending an existing approximate analysis. In this section, we first describe briefly a framework that has been used to predict and interpret the characteristics of linear and nonlinear oscillations in combustion chambers. We then indicate how that analysis may be applied to the problem of pollution. It is an intrinsic property of this approach that careful modeling and explicit calculations of contributing physical processes are prerequisite to obtaining quantitative global results. The discussion in this section suggests what processes must be accommodated and where they fit in the approximate analysis.

Formulation of the analysis begins with the conservation equations of mass, momentum and energy. To those we must eventually add equations governing the time and spatial evolution of chemical species, and a set of equations representing the kinetic mechanism. The analysis is concerned essentially with matters of coupling between unsteady fluid motions and the chemical processes. In the framework

constructed here, the coupling or interactions are strongly biased in one direction. The unsteady motions (i.e. the pressure, temperature and velocity fluctuations) determine unsteady formation of chemical species, but are themselves weakly influenced by the detailed chemistry. Here we ignore the latter, to concentrate on a method for calculating the time-dependent formation of chemical species in a combustor. Of course, the comparable assumption cannot be made with respect to steady motions: the flow itself depends on the production of energy released in chemical reactions; even for steady flow much useful information is gained even with quite severe approximations to the chemistry. In analysis of the unsteady flows we assume that the properties of the steady flow are known.

Much of the formulation may therefore be constructed without regard for the species equations and begins with the equations for the conservation of mass, momentum and energy written in the primitive form.

MASS
$$\frac{\partial \rho}{\partial t} + \nabla \cdot (\rho \mathbf{u}) = \mathtt{W} \tag{1}$$

MOMENTUM
$$\frac{\partial}{\partial t}(\rho \mathbf{u}) + \nabla \cdot (\rho \mathbf{u}\mathbf{u}) + \nabla p = \nabla \cdot \tau + \mathbf{F} \tag{2}$$

ENERGY
$$\frac{\partial}{\partial t}(\rho e_0) + \nabla \cdot (\rho \mathbf{u} e_0) + \nabla \cdot (\rho \mathbf{u}) = \nabla \cdot (\tau \cdot \mathbf{u}) + \nabla \cdot \mathbf{q} + Q + \mathbf{u} \cdot \mathbf{F} \tag{3}$$

where $\rho$, $\mathbf{u}$ and p are the density, velocity and pressure; $e_0 = e + u^2/2$ is the stagnation internal energy ($de = C_v dT$ where T is temperature); $\tau$ is the viscous stress tensor; $\mathbf{q}$ is internal heat transfer; and $\mathtt{W}$, $\mathbf{F}$ and Q represent sources of mass, momentum and energy, the last being essentially the heat released in chemical reactions. The equation of state is

$$p = \rho R T \tag{4}$$

Standard manipulations of these equations lead to the set

$$\frac{D\rho}{Dt} = -\rho \nabla \cdot \mathbf{u} + \mathtt{W} \tag{5}$$

$$\rho \frac{D\mathbf{u}}{Dt} = -\nabla p + F \tag{6}$$

$$\rho C_\upsilon \frac{DT}{Dt} = -p \nabla \cdot \mathbf{u} + \mathtt{Q} \tag{7}$$

$$\frac{Dp}{Dt} = -\gamma p \nabla \cdot \mathbf{u} + \mathcal{P} \tag{8}$$

$$T\frac{Ds}{Dt} = \mathcal{Q} - RT\mathcal{W} \tag{9}$$

where,

$$\mathcal{F} = \nabla \cdot \boldsymbol{\tau} + \mathbf{F} - \mathbf{u}\mathcal{W} \tag{10}$$

$$\mathcal{Q} = (\boldsymbol{\tau} \cdot \nabla) \cdot \mathbf{u} + \nabla \cdot \mathbf{q} + \mathcal{Q} - \left(e - \mathbf{u}^2 / 2\right)\mathcal{W} \tag{11}$$

$$\mathcal{P} = \frac{R}{C_v}\left(\mathcal{Q} + C_v T\mathcal{W}\right) \tag{12}$$

So far as combustion instabilities in a gas turbine are concerned, the contributions from $\mathcal{F}, \mathcal{W}, \boldsymbol{\tau}$ and $\mathbf{q}$ are normally negligible, giving the simple result for $\mathcal{P}$,

$$\mathcal{P} = R\mathcal{Q}/C_v = R\mathcal{Q}/C_v \tag{13}$$

Nonlinear gas dynamic processes are important in the kinds of problems envisioned here, acting to couple the turbulent and acoustic fields [11,12]. Experience with analysis of nonlinear combustion instabilities has demonstrated that it is sufficient to carry nonlinear contributions to second order: third order terms seems to generate only quantitative, not qualitative, corrections. The flow field is represented as a sum of a steady mean field and an unsteady fluctuation, $p = \bar{p} + p'$, $\mathbf{u} = \bar{\mathbf{u}} + \mathbf{u}'$, etc. For simplicity here we will assume $\bar{p}$, $\bar{\rho}$ and $\bar{T}$ uniform but $\bar{\mathbf{u}}$ must be non-uniform.

The next step in the formulation is construction of a nonlinear wave equation for the pressure fluctuation and its associated boundary condition, i.e.

$$\begin{aligned} &\nabla^2 p' - \frac{1}{a^2}\frac{\partial^2 p'}{\partial^2} = h \\ &\hat{n} \cdot \nabla p' = -f \end{aligned} \tag{14a,b}$$

with $a^2 = \gamma\, \bar{p}/\, \bar{\rho}$. Details of the derivation and the formulas for h and f may be found in the references cited above; they are unimportant in the present discussion.

Application of a form of Galerkin's method, a convenient way of spatially averaging the governing equations (14) a,b, produces the set

$$\ddot{\eta}_n + \omega_n^2 \eta_n = \mathrm{F}_n \tag{15}$$

where

$$F_n = -\frac{a^2}{\bar{p}E_n^2}\left\{\int h\psi_n dV + \oiint f\psi_n dS\right\}$$
$$E_n^2 = \int \psi_n^2 dV \tag{16}$$

The $\psi_n(\vec{r})$ are the eigenfunctions for the unperturbed classical acoustic problem set in the same geometry as the combustion chamber in question; $\omega_n = ak_n$ is the frequency of the $n^{th}$ normal mode and $k_n$ is the wavenumber. Derivation of (15) for the amplitudes $\eta_n$ rests on spatially averaging (14)a,b after substituting the series representation of the pressure field,

$$p' = \bar{p}\sum_{j=1}^{\infty}\eta_j(t)\psi_j(\vec{r}) \tag{17}$$

With the approximation to second order noted above, the forcing function $F_n$, defined by (16), can eventually be written

$$-\frac{\bar{p}E_n^2}{a^2}F_n = \bar{\rho}I_1 + \frac{1}{a^2}I_2 + \bar{\rho}I_3 + \frac{1}{a^2}I_4 + \oiint\bar{\rho}\frac{\partial \mathbf{u}'}{\partial t}\cdot\hat{n}dS - \int\frac{1}{a^2}\frac{\partial P'}{\partial t}\psi_n dV \tag{18}$$

where,

$$I_1 = \int(\bar{\mathbf{u}}\cdot\nabla\mathbf{u}' + \mathbf{u}'\cdot\nabla\bar{\mathbf{u}})\cdot\nabla\psi_n dV$$
$$I_2 = \frac{\partial}{\partial t}\int(\gamma p'\nabla\cdot\bar{\mathbf{u}} + \bar{\mathbf{u}}\nabla\cdot p')\psi_n dV$$
$$I_3 = \int\left(\mathbf{u}'\cdot\nabla\mathbf{u}' + \frac{\rho'}{\bar{\rho}}\frac{\partial \mathbf{u}'}{\partial t}\right)\cdot\nabla\psi_n dV \tag{19}a,b,c,d$$
$$I_4 = \frac{\partial}{\partial t}\int(\gamma p'\nabla\cdot\mathbf{u}' + \mathbf{u}'\nabla\cdot p')\psi_n dV$$

In deriving these formulas for the integrals $I_1$-$I_4$, some use has been made of the classical acoustics relations, $\bar{\rho}\mathbf{u}_t' = -\nabla p'$ and $p_t' = -\gamma\bar{p}\nabla\cdot\mathbf{u}'$, a step consistent with the order to which the equations have been written. The approximation can be justified by carrying out a two-parameter expansion of the original conservation equations, the two small parameters being Mach numbers characterizing the steady and unsteady fields.

A significant feature of the general problem defined by (15), (16), (18) and (19) is that the influences of a turbulent reacting flow on acoustic waves can be determined simultaneously with the noise field. The analysis supporting that statement is in progress and will be described but briefly here. The

fundamental idea is that developed most completely by Chu and Kovasznay [13], that any disturbance in a compressible flow can be treated as a synthesis of three 'modes' of propagation, or classes of waves: acoustic, vortical, and entropic (or temperature) waves. In the linear limit, these three modes of propagation possess the following fundamental properties not proved here: (i) pressure fluctuations are carried only by acoustic waves which propagate with the speed of sound a; (ii) vortical and entropic disturbances are carried by the mean flow and hence propagate with the local mean flow velocity; and (iii) vorticity and entropy fluctuations are associated respectively with vortical and entropic waves only.

The fluctuations of pressure, vorticity and entropy (or nonisentropic temperature) are nonzero only for their corresponding modes of propagation. An immediate consequence is that coherent acoustic waves and the noise field can be represented, at least in principle, by the synthesis (17) of classical normal modes. Development of this idea requires lengthy formal calculations [11,12] leading finally to the more explicit form for the set of coupled oscillator equations,

$$\ddot{\eta}_n + \omega_n^2 \eta_n = \alpha_n \eta_n + \theta_n \dot{\eta}_n + \mathrm{F}_n^{NL} + \xi_n \eta_n + \xi_n^v \dot{\eta}_n + \sum_{i=1}^{\infty} \left[ \xi_{ni} \eta_i + \xi_{ni}^v \dot{\eta}_i \right] + \Xi_n \qquad (20)$$

Here $F_n^{NL}$ stands for the well-known terms arising from second-order nonlinear gasdynamics (see ref. [2], for example) and the $\xi_n(t)$, $\xi_n^v(t)$, ..., $\Xi_n(t)$ represent stochastic processes responsible for the background noise evident in experimental data. They are defined in terms of the integrals (19) a,b,c,d with the velocity fluctuation replaced by its values for one of the three modes of propagation. Thus, the first term in $I_3$ gives rise to nine distinct integrals which contribute to the stochastic functions in (20).

## Coupling of Unsteady Motions with Chemical Kinetics

The formulation described in the preceding section leads to the representation (20) of the unsteady pressure field as a collection of nonlinear oscillators driven by energy released by chemical reactions, coupling with the mean flow field, and interactions with the turbulence field. Nearly all published works on combustion instabilities neglect the influences of turbulence and are concerned with stability of small disturbances and some aspects of nonlinear behavior. The details of the chemistry are buried in representations of the unsteady heat release and normally receive little attention, although that omission is being corrected in recent works on unsteady burning of solid propellants.

As we remarked earlier, we assume here that the unsteady motions can be computed (i.e. by solving the set (20)) without specifying details of the chemistry. That assumption implies assigning the fluctuation Q′ of heat release values that depend only on the velocity and thermodynamic variables. Having, in principle, determined the unsteady field, we then turn attention to its influence on the chemical kinetics required to describe the formation of pollutants - here nitrogen oxides. Each of the species, having concentration $Y_i = \rho_i/\rho$ is described by the equation

$$\frac{\partial Y_i}{\partial t} + \rho \mathbf{u} \cdot \nabla Y_i = \nabla \cdot \left( \rho D \nabla Y_i \right) + w_i \tag{21}$$

where $w_i$ is the production rate, having dimension $s^{-1}$.

Given the unsteady field (p′, ρ′, T′ and **u**′) and a formula for the source $w_i'$ in terms of the field variables, the formation of species is to be computed by solving the set (21) written for the fluctuations. Presently there is no formal approximate method for doing so and solutions must be obtained numerically. That procedure would then give the global distributions of the $Y_i'$ and the rates at which the species depart the chamber. A complete treatment of the problem must also include computation of nonisentropic temperature fluctuations which are lightly coupled (in both directions) to the species concentrations; we ignore that problem here.

The remainder of this paper is concerned with only a small but important part of the general problem just described, namely fluctuations $w_i'$ of the local production rate of constituent i when the unsteady field is specified. We examine several simplified elementary modes of the kinetic mechanism as a means of investigating the response of the chemical kinetics to imposed oscillations. The results amount to an initial determination of models of the local "response function" for the reacting system. Such a response function could then be used as a representation of $w_i'$. We are far from carrying out the program suggested by the preceding discussion which here serves chiefly to provide the context for the calculations given in the following sections.

## Numerical Results for Complete Chemistry Simulations

The first method employed to determine the behavior within a gas turbine combustor is the use of PSR (perfectly stirred reactor) and PFR (plugged flow reactor) modules to break up the flow field into simplified elements and make accurate determinations of the chemistry. The results from the numerical simulations and experimental results provide guidelines as to how the combustion chamber can be broken up into elements that approximate different flame zones. This division of the chamber into regions of PSR and PFR elements is useful for investigating the overall chemistry production in the context of an extremely simplified form of the complex flow field. This work has been very useful in the determination of pollutant emissions where conventional experimental methods might not be usable, for example in the main flame zone of a combustion chamber.

Most applications of the PSR and PFR elements involve steady state calculations of the species field. While these results are useful, they might not accurately portray the behavior of the reaction rates in the presence of nonlinear oscillations and noise which affect real combustors. It was for this reason that Feitelberg [14] began work to impose an oscillating condition onto a PSR element and look at how the pressure, temperature and species mass fractions were related. The results Feitelberg presented showed an increase in the average amount of NOx produced under oscillating conditions. Since a PSR was used, this simulation models the main flame zone behavior only or a small region of a combustor. Due to the exponential dependence of the NOx production rate on the temperature field, it should be no surprise that an oscillating temperature field with a constant T′ led to a oscillating NOx production with more NOx produced while the temperature was cycling above the mean value than NOx reduction while the temperature was cycling below the mean value.

Work along this line of reasoning has been continued as a part of this program. As a first step the work has been based on a configuration of PSR and PFR elements intended to simulate the behavior of NOx levels at various locations within a given chamber design. The given setup is run at a series of steady state conditions by varying the input equivalence ratio. The steady state results are then used to develop a correlation between the temperature levels and the pollutant levels at the exit plane of each element. Earlier work was performed with varying pressure values as well, but it was determined that the pollutant levels will depend weakly on the pressure and strongly on the temperature for the fluctuation range we are concerned with. Due to this, only temperature dependence will be described here.

Figure 1 is a sketch of the actual gas turbine combustor geometry simulated in this paper. It should be noted that the sketch is an axisymmetric slice of the chamber and is not drawn to scale. Figure 2 shows the way in which the combustor geometry was divided into a system of PSR and PFR elements. The impact of the pilot flame was neglected and replaced with a PFR recirculation element. The Miller-Bowman mechanism [15] was used to determine the chemical kinetics for the reactions. The method for determining dynamic behavior was different from the method used by Feitelberg. Feitelberg imposed a fluctuation in the upstream pressure at distinct time intervals in a continuous manner. This method made use of the current state in the PSR for future calculations. The method used for this paper was even more quasi-steady in nature. A separate simulation, started from baseline initial conditions, was run for a series of distinct equivalence ratio input conditions. These separate simulations were used to correlate a curve of species concentrations of NOx and CO to the temperature. Figure 3 shows the distinct point values and the curve fits for the NOx and CO levels at the exit of elements PSR2 and PFR4. The relations for the NOx dependence on temperature for the exit of elements PSR2 and PFR4 are given by:

$$\begin{aligned} [\mathrm{NOx}(15\%\mathrm{Dry})] &= 14.37\mathrm{T}^{1.905}\, exp\left(-2.622\mathrm{E}4/\mathrm{T}\right) \qquad \text{at PSR exit} \\ [\mathrm{NOx}(15\%\mathrm{Dry})] &= 52.99\mathrm{T}^{2.149}\, exp\left(-3.059\mathrm{E}4/\mathrm{T}\right) \qquad \text{at system exit} \end{aligned} \tag{22a,b}$$

The mole fraction of CO for these same regions was fit using a polynomial to fifth power in temperature.

An oscillation of the temperature field was then imposed on these relations determined from the distinct steady state simulations. At each point along the temperature oscillation, the NOx and CO values were determined from the curve fit. The oscillation values were determined for one period and the average values of the NOx and CO levels were determined over this cycle. Figures 4 and 5 show the NOx and CO levels along with the temperature for one period of the oscillation for elements PSR2 and PFR4. The average values are also shown in the figure. The temperature oscillation used was a 2 percent variation around the mean value of 1624 K in element PSR2 and 1597 K in PFR4. As can be seen from the figures, the pollutant levels at both exit planes are increased in the presence of a temperature oscillation. Our use of a quasi-steady application of an oscillating temperature field to steady state relations between the chemical species and temperature was compared to Feitelberg's method of imposing an oscillation which made better use of the time history within a PSR to determine dynamic response. The main result shown by Feitelberg [14] involved a 2% temperature oscillation. He showed that the average NOx level in the

presence of this oscillation showed an increase of 2.3%. Our result for the same oscillation level and using equation 22a, showed an increase of 2.5% in the average NOx level. Although it is only one matching condition, it seems that these two approximate methods are comparable and may provide a qualitative description of how pollutant levels will change within a single PSR or PFR element.

Since, this is only an initial step to determine how chemistry behaves with an oscillating flow and the PSR, PFR system is already a crude approximation, we believe these approximations are acceptable to provide a qualitative idea of the effects of an oscillating field. However, since the PSR and PFR method for chemistry determination does not accommodate dynamic behavior in a rigorous way, research in this area might provide a way of determining accurate levels and qualitative dependence on temperature, but will not provide much insight into the system wide dynamic response between the chemical species and an unsteady flow field.

**Numerical Results for Complex Geometry Simulations**

The other method being used to investigate the nonlinear behavior within a gas turbine combustor is based on solving the fluid flow with a limited chemical reaction system and with a grid system that matches the complex geometry of an actual combustor. Since the fluid flow is already a complicated and sometimes stiff problem to solve, the complexity of the chemical reactions is reduced in order to lessen computational time and to keep the overall system from being too complex to solve. The numerical simulation of the entire flow field is a widely sought goal in the research field. It is intended to improve the research and design capabilities of the gas turbine industry by reducing the cost associated with experimental firings and increasing the amount of information that can be determined about the flow field and flame structure of a given system. There has been much progress in the area of steady state calculations for full scale combustors [16-18]. Beyond steady state simulations, work towards transient simulations is also underway [19-21]. This work on transient simulations should provide better information about interactions between the flow field and the reaction rate chemistry. The results will also provide a framework for testing control schemes to help damp out nonlinear oscillations.

The work conducted for this paper was first designed to simulate the steady state behavior for a gas turbine combustor. The idea is then to use those results to examine the transient behavior within the combustion chamber. The numerical calculations were performed using the commercially available code ANSWER developed by ACR, Inc. The code is a full Navier-Stokes solver making use of the ADI (alternating direction implicit) scheme to solve for the complete flow field variables. The turbulence was calculated via a k-ε model and the EBU (eddy-breakup model) was used in the reaction rate determination. The chemistry rates were simplified to a 3-step methane reaction:

$$\begin{aligned} CH_4 + \tfrac{3}{2}O_2 &\rightarrow CO + 2H_2O \\ CO + \tfrac{1}{2}O_2 &\leftrightarrow CO_2 \end{aligned} \qquad (23)$$

A 5-step method, with the inclusion of NOx production, was not available for the work performed for this paper but will be implemented in further studies to determine how nonlinear behavior affects the NOx production in various regions of the chamber.

The gas turbine combustor modeled is intended for use in stationary power plant applications. In order to simplify the simulation even further, the flow was modeled as a 2-D axisymmetric system as can be seen in figure 1. The combustor has both a premixed flame and a central pilot flame which are both run in lean conditions. The inlet temperature was set as 650 K and the reference pressure was set as 14e5 Pa. Secondary air flow was input tangentially along the top of the chamber.

Figure 6 shows the grid employed. Note that the scale along the y-axis has been magnified to better show the details of the field. The letter markers will be used in the other graphs to indicate where the history results have been determined. Figure 7 is a contour of the steady state temperature field. Figure 8 shows the steady state velocity contour. The central recirculation zone is very distinct in this plot. The simulation also calculated the tangential velocity in order to look at any affects of swirl on the steady state and transient results. These steady state values will be important for further nonlinear analysis of acoustic interactions within the chamber by the use of the analytical tools mentioned earlier in the paper. The temperature field can be used to determine the acoustic frequency modes and mode shapes for the chamber.

The steady state results provided a starting point for the transient calculations. In order to initiate oscillations in the chamber, two methods were used. The first method was a simple velocity pulse at the

pilot air inlet. This pulse corresponds to a mass flow pulse which will be convected downstream at a rate proportional to the local velocity. In order to have smooth transitions into and out of the pulse, the form of the pulse was taken as:

$$U(t) = U_o + \frac{16\Delta U}{\tau^4} t^2 (t-\tau)^2 \qquad (24)$$

The first method was designed to trigger any nonlinear self sustained oscillations within the chamber. The results for the conditions used showed a transition within the flame structure, but no sustained oscillations. The second method was intended to drive the oscillations at a given frequency to see if a resonance state occurred and also check how flow field variables interacted locally. The oscillation was initiated with a pulse up until $t = \tau/2$ where $\tau$ had the same definition as in (24) and then a cosine function with respect to time was employed.

Figure 9 shows the axial velocity that was imposed at the air inlet of the pilot section. Figures 10 and 11 show the time history of various values of the flow field for a point in the center of the diffusion flame, point B in figure 6, and at a point in the center of the recirculation zone, point E in figure 6. After some initial start up time, the imposed inlet oscillation has led to the development of a oscillation within the chamber. The imposed oscillation was at a frequency of 100 Hz and the downstream oscillation showed a frequency around 100 Hz. The simulation with the simple pulsed inlet condition showed similar start up behavior and transition to a secondary state, but no sustained oscillations were developed. Figures 12 and 13 show phase plots at points B and E within the chamber. These relations can be used in the nonlinear analysis to attempt to model how the pressure and velocity interact locally, as well as how the chemistry field will interact with the temperature.

The plots of axial velocity versus the relative pressure show that, locally and in the limit cycle, these variables are in phase with each other. One of the main concerns in nonlinear combusting flow is how the heat release is coupled with the pressure field. According to Rayleigh's criterion, if the integral of these terms over the entire chamber is positive, there will be a driven system. In order to approximate the heat release rate, it was assumed here to be related to the time variation of the temperature. Figures 14 and 15 show the phase plots versus this time variation of temperature for points B and E. At these points, the pressure and the term related to heat release are in phase with each other and local driving should take

place. Of course, this local driving may be overcome by acoustic damping within the rest of the chamber and an overall unsteady situation may not develop.

The other important modeling tool to be determined from this research is the dependence of the species production on the temperature and other flow field quantities. The flow variable of greatest concern is the temperature, although velocity will also be important for local diffusion and convection determination. Similarly with the heat release rate, the variation in the chemical production terms was assumed to be related to the time variation of the mass fractions of the chemical species. Figures 16 and 17 show the plots of the time variation of $CH_4$ and CO versus temperature. The CO plots will give good indication how the production rate will be affected by an oscillating temperature field. However, since the $CH_4$ is actually being burned away, this correlation will be more important in describing the local rate of destruction.

## Conclusions

The work presented in this paper was designed as a preliminary analysis of how to develop dynamic response models between flow field variables and chemical production rates. The results described were designed to give some framework for the development of these dynamic response models. The PSR and PFR results demonstrated an ability to accurately calculate the levels of chemical species in steady state operation. Fitting curves to these steady state results can provide some guide as to proper pollutant level dependence in future dynamics work; however, a system of these PSR and PFR elements does not appear to have the dynamic flexibility for detailed transient simulations which are needed for proper phase information.

The detailed geometry simulation results have shown that they can handle transient solutions and are therefore more likely to provide the information necessary for good local and global dynamic response models. The results have shown the ability to investigate overall nonlinear effects, by examining how the pressure and the velocity, or the pressure and the heat release are coupled in time. The results have also shown that the transient simulations can provide local relations between the chemical production terms and the temperature, which will be of further use in developing dynamic response models to describe the

complete system. The addition of more detailed chemistry in this analysis in the future will provide a more detailed transient simulation to use for dynamic response modeling.

**Acknowledgment:**

This work was partially supported by the California Institute of Technology; and by CRTN-ENEL, Pisa, Italy (Dr. G. Benelli, program manager).

**References**


1. Culick, F.E.C. (1988) "Combustion Instabilities in Propulsion Systems," AGARD Conference Proceedings, Paper 1, 450.

2. Culick F.E.C. (1994) "Some Recent Results for Nonlinear Acoustics in Combustion Chambers," AIAA Journal 32:146-169.

3. Culick F.E.C. and Yang V. (1992) "Prediction of the Stability of Unsteady Motions in Solid Propellant Rocket Motors," AIAA Progress in Aeronautics and Astronautics Series 143:719-779.

4. Culick F.E.C., Paparizos L., Sterling J. and Burnley V. (1991) "Combustion Noise and Combustion Instabilities in Propulsion Systems," AGARD Conference on Combat Aircraft Noise, AGARD CP 512.

5. Correa S.M. (1992) "A Review of NOx Formation Under Gas-Turbine Combustion Conditions," Combustion Science and Technology 87:329-362.

6. Rizk N.K. and Mongia H.C. (1993) "Semi-analytical Correlations for NOx, CO and UHC Emissions," Journal of Engineering Gas Turbine and Power, Transactions of the ASME 115:612-619.

7. Newburry D.M. and Mellor A.M. (1995) "Characteristic Time Model Correlation of NOx Emissions from Lean Premixed Combustors," ASME Paper No. 95-GT-135.

8. Leonard G. and Correa S. (1990) "NOx Formation in Premixed High-Pressure Lean Methane Flames," Fossil Fuels Combustion Symposium.

9. Keller J.O. and Hongo I. (1990) "Pulse Combustion: The Mechanisms of NOx Production," Combustion and Flame 80:219-237.

10. Correa S.M. and Shvy W. (1987) "Computational Models and Methods for Continuous Gaseous Turbulent Combustion," Progress in Energy and Combustion Science 13:249-292.

11. Culick F.E.C. (1995) "Nonlinear Acoustics in Combustion Chambers with Stochastic Sources," Jet Propulsion Center Document CI95-6, California Institute of Technology.

12. Burnley V. (1996) "Nonlinear Combustion Instabilities and Stochastic Sources," Ph.D. Dissertation, Department of Aeronautics, California Institute of Technology.

13. Chu B.-T. and Kovasznay S.G. (1958) "Non-Linear Interactions in a Viscous Heat-Conducting Compressible Gas," Journal of Fluid Mechanics 3:494-514.

14. Feitelberg, A. S. (1995) "The Perfectly Stirred Pulsed Reactor," Eastern States section meeting of the Combustion Institute, Wercester Polytechnic Institute 217-220.

15. Miller J.A. and Bowman C.T. (1989) "Mechanism and Modeling of Nitrogen Chemistry in Combustion," Progress in Energy Combustion Science 15:287-338.

16. Rizk N.K. and Mongia H.C. (1993) "Three-Dimensional Gas Turbine Combustor Emissions Modeling," Journal of Engineering Gas Turbine and Power, Transactions of the ASME 115:603-611.

17. Di Martino, P., Cinque, G., Paduano, C., and Cirillo, L. (1994) "Numerical Study of Swirling Reacting Flow in a Can-Type Combustor," AIAA Paper No. AIAA-94-3044.

18. Dupoirieux, F. and Desaulty M. (1995) "A Coherent Research Effort on Combustion: The A3C Operation."

19. Kailasanath, K., Gardner, J. H., Oran, E. S., and Boris, J. P. (1991) "Numerical Simulations of Unsteady Reactive Flows in a Combustion Chamber," Combustion and Flame 86:115-134.

20. Benelli, G., Cossalter, V., and Da Lio, M. (1993) "Advances in Numerical Simulation of Pulsating Combustion at ENEL," Combustion Science and Technology 94:317-335.

21. Liu, R. and McGuirk, J. J. (1995) "Prediction of Combustion Induced Oscillations using a Pressure-Correction Method," ASME paper no. 95-GT-336.

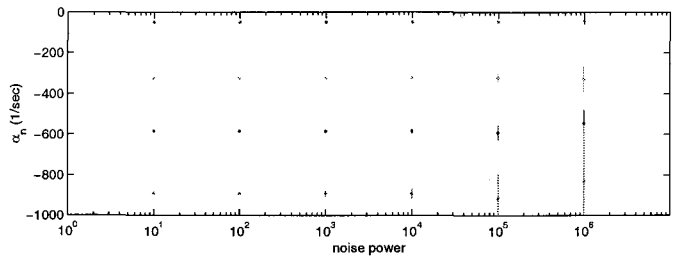


| Noise | $\alpha_1$ | $\alpha_2$ | $\alpha_3$ | $\alpha_4$ |
|---|---|---|---|---|
| $10^1$ | -50±1 | -325±1 | -584±2 | -891±3 |
| $10^2$ | -50±1 | -325±1 | -585±2 | -891±5 |
| $10^3$ | -50±1 | -325±2 | -585±4 | -894±8 |
| $10^4$ | -49±2 | -323±3 | -584±10 | -891±21 |
| $10^5$ | -47±6 | -323±16 | -592±35 | -916±119 |
| $10^6$ | -42±17 | -327±62 | -544±65 | -831±274 |
| correct | -50 | -325 | -584 | -889 |

Figure 11: Decay rates detected using the method of pulsing.

increases dramatically as the decaying pressure pulse gets rapidly 'drowned' by the noise. This effect is especially pronounced for the fast decaying higher modes and is in sharp contrast to the independence of the identification accuracy using the power spectrum. Using this latter method the values of all decay constants can be given to 20% uncertainty for any noise level.

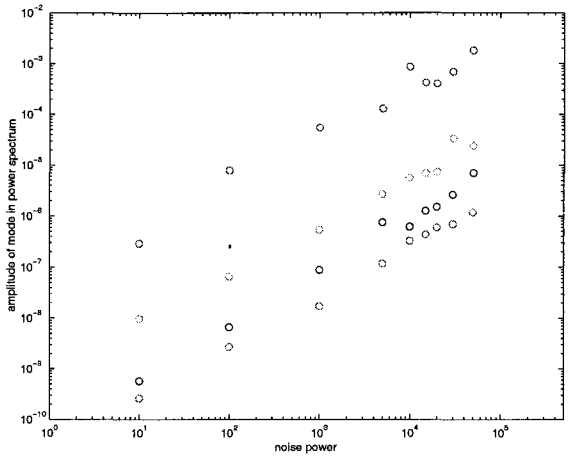


Figure 12: Peak amplitudes for all modes in the power spectral density vs. input noise power

## 4.2 Linear motions with multiplicative noise

The numerical experiments are repeated for multiplicative noise. A certain amount of additive noise (noise power $10^4$) is also added to excite the otherwise stable system.

There are two distinct kinds of multiplicative noise; in equation (37) they are denoted by $\xi^v$ and $\xi$, causing respectively stochastic fluctuations of the damping and the frequency. Both kinds of source terms are analyzed separately.

Figures 13 and 14 show the effect of random perturbations of the frequency shift on the identified decay rates of the individual modes using the two different methods. No apparent effect is noticeable – both the mean value and the uncertainty associated with it remain unaffected by the noise source. Comparing with

**Captions for Figures**

Figure 1 - Sketch of Gas-Turbine Combustor used for Simulations (Not to Scale)

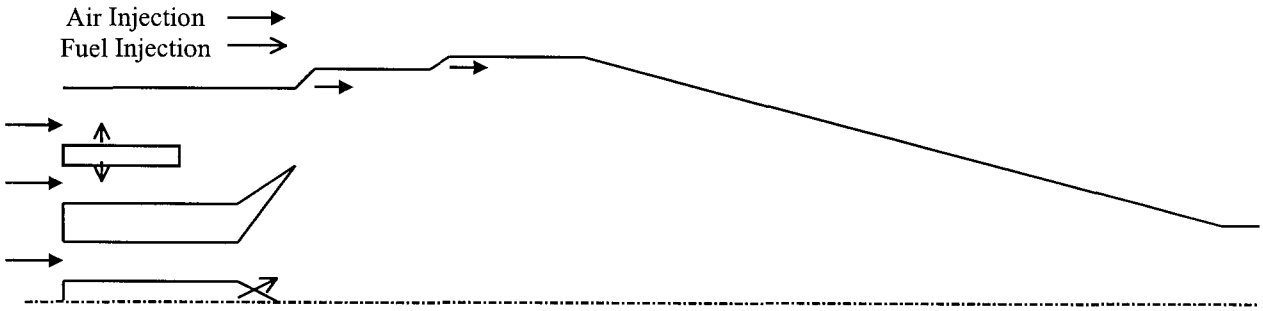


Figure 2 - Sketch of PSR and PFR System

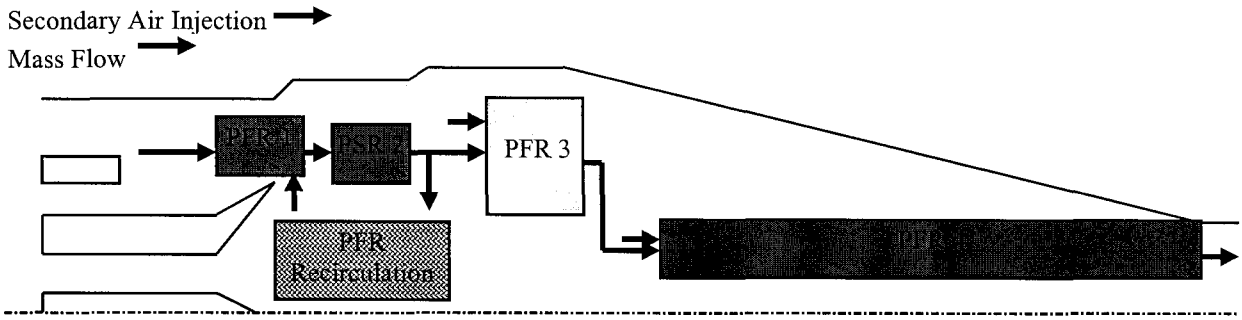


Figure 3 - Steady State PSR and PFR Results for NOx and CO versus Temperature

Figure 4 - Imposed Temperature Oscillation at Exit of Element PSR2 - NOx and CO Levels

Figure 5 - Imposed Temperature Oscillation at Exit of Element PFR4 - NOx and CO Levels

Figure 6 - 2D Grid Used for Numerical Simulations; Letters Denote Transient History Recording Points

Figure 7 - Steady State Temperature Contour for Gas-Turbine Combustor

Figure 8 - Steady State Axial Velocity Contour for Gas-Turbine Combustor

Figure 9 - Imposed Oscillating Axial Velocity versus Time at Point A: the Pilot Air Inlet

Figure 10 - Time History Curves of U, P, T, CO at Point B: Center of Diffusion Flame

Figure 11 - Time History Curves of U, P, T, CO at Point E: Center of Recirculation Zone

Figure 12 - Phase Plots at Point B: $CH_4$ Mass Fraction versus Temperature; Axial Velocity versus Pressure

Figure 13 - Phase Plots at Point E: $CH_4$ Mass Fraction versus Temperature; Axial Velocity versus Pressure

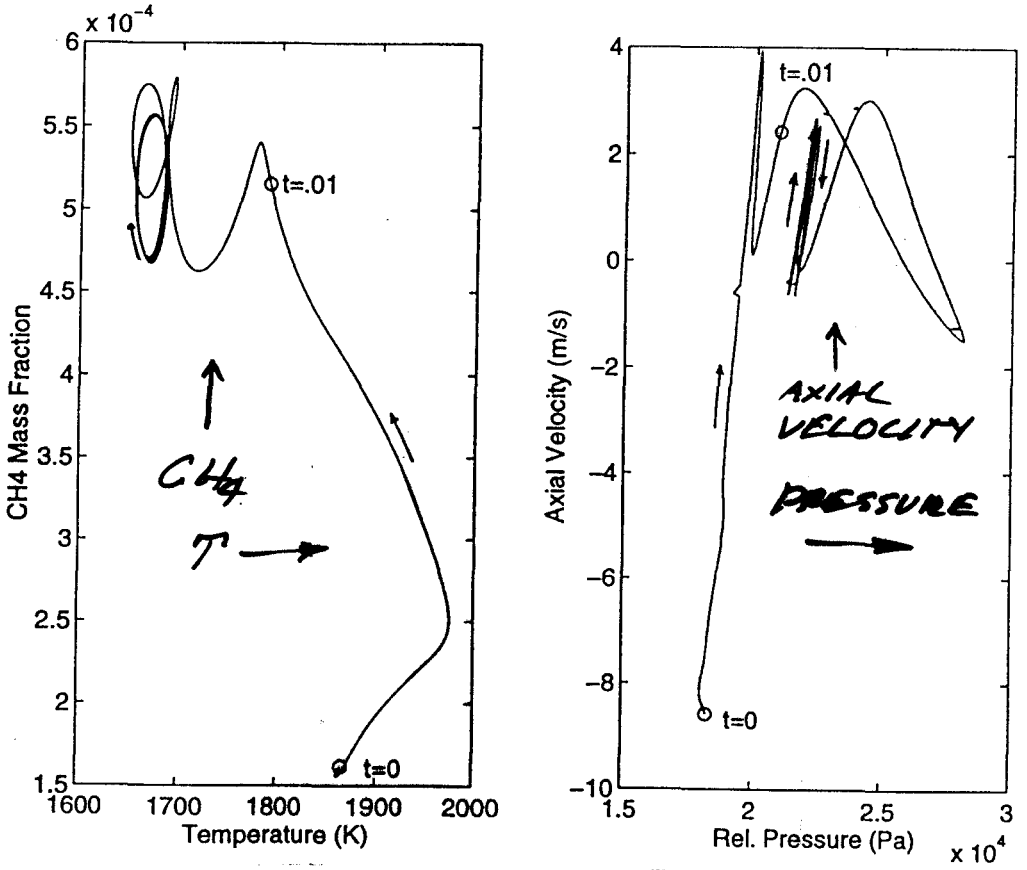


Figure 12 - Phase Plots at Point B: $CH_4$ Mass Fraction versus Temperature; Axial Velocity versus Pressure

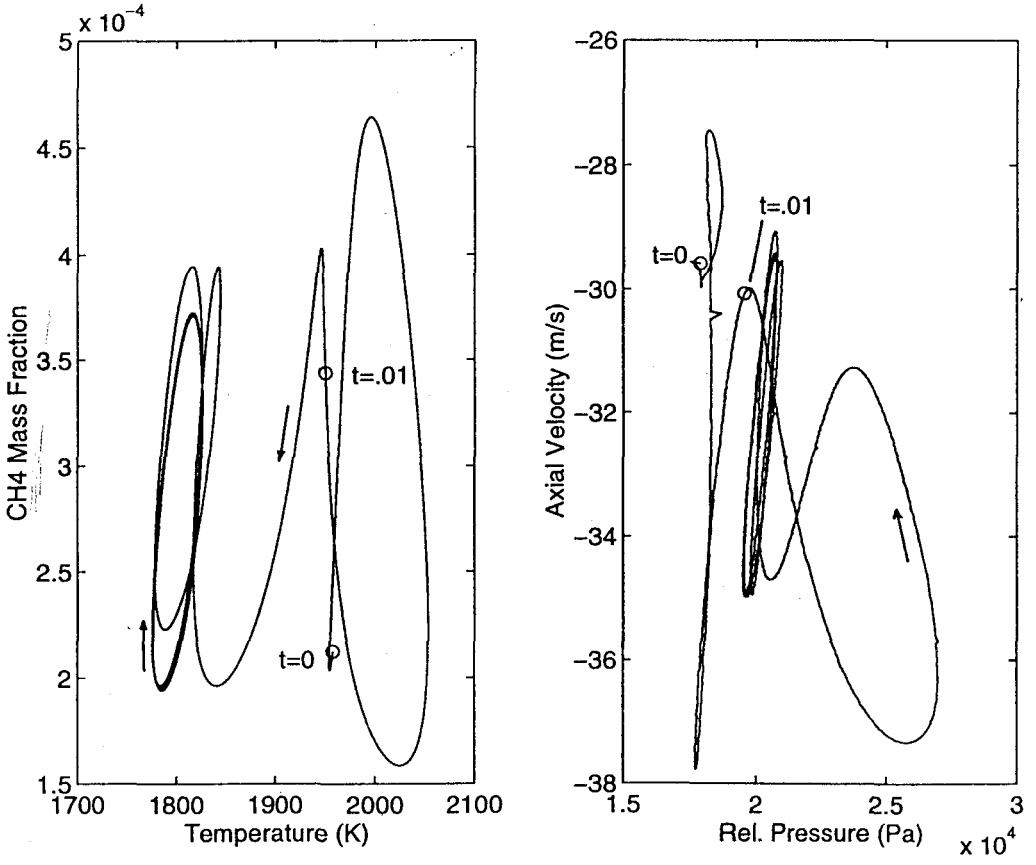


Figure 13 - Phase Plots at Point E: $CH_4$ Mass Fraction versus Temperature; Axial Velocity versus Pressure

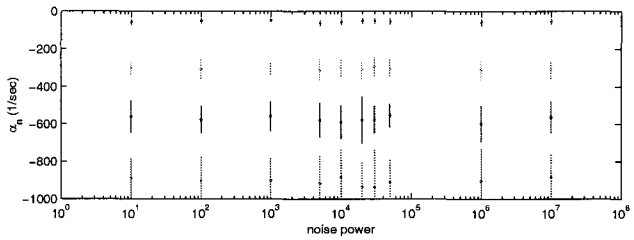


| Noise | $\alpha_1$ | $\alpha_2$ | $\alpha_3$ | $\alpha_4$ |
|---|---|---|---|---|
| $10^1$ | -57±14 | -301±31 | -560±84 | -886±98 |
| $10^2$ | -51±13 | -307±52 | -576±75 | -903±126 |
| $10^3$ | -47±11 | -307±38 | -558±78 | -901±117 |
| $10^4$ | -56±16 | -300±51 | -591±88 | -883±150 |
| $10^5$ | -59±18 | -310±53 | -598±95 | -914±128 |
| $10^6$ | -53±15 | -310±46 | -564±84 | -905±172 |
| $10^7$ | -59±19 | -313±44 | -591±83 | -887±124 |
| correct | -50 | -325 | -584 | -889 |

Figure 13: Decay rates by Burg's method in the presence of multiplicative $\xi$ noise (frequency shift perturbations)

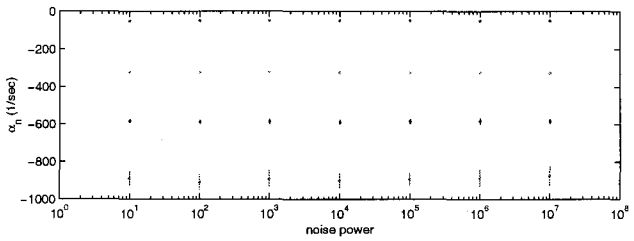


| Noise | $\alpha_1$ | $\alpha_2$ | $\alpha_3$ | $\alpha_4$ |
|---|---|---|---|---|
| $10^1$ | -50±2 | -323±6 | -584±9 | -889±35 |
| $10^2$ | -50±2 | -325±5 | -589±8 | -908±36 |
| $10^3$ | -50±2 | -322±4 | -587±10 | -891±44 |
| $10^4$ | -50±3 | -326±5 | -589±8 | -902±37 |
| $10^5$ | -49±3 | -326±4 | -586±12 | -895±35 |
| $10^6$ | -50±2 | -324±4 | -582±15 | -886±43 |
| $10^7$ | -49±3 | -327±4 | -583±11 | -877±51 |
| correct | -50 | -325 | -584 | -889 |

Figure 14: Decay rates by the method of pulsing in the presence of multiplicative $\xi$ noise (frequency shift perturbations)

the previous section, it can be seen that the observed scatter is only due to the presence of the additive noise.

At the same time the identification (mean and accuracy) of the modal frequencies (and thus of the frequency shifts) is independent of this sort of parametric noise. This is due to the fact that the length of the analyzed pressure trace is much longer then the fundamental period and therefore the frequency perturbations average out.

The influence of growth rate perturbations is displayed in figures 15 and 16. At low levels the system identification based on Burg's method gives the same results in terms of mean detected growth rates and their uncertainty as for the other types of noise. As the noise level grows, however, a shift in the mean values occurs (and thus a wrong determination of the system parameters!), paired with a spreading uncertainty. Finally, as the noise power reaches a critical level the linear system ID process breaks down.

This type of parametric noise also strongly affects the identification of the system parameters determined by measuring the decaying pulse in the chamber. It should be noted that even at the low noise levels where Burg's method delivered familiar results, the method of pulsing shows rather large standard deviations (25% for the first mode) of the detected parameters when compared with low levels of the other kinds of pertubations (where the error was of the order of 1%). With growing noise level both shifts of the mean values (growing identification error) and a ballooning uncertainty are apparent before the identification process completely fails.

At this 'break-down point' the instantaneous growth rate of the first mode (the least stable one) has a finite probability of being positive thus changing the qualitative behavior of the system. As a result the system response undergoes a dramatic change: the pressure signal now exhibits 'spontaneous bursts'. This phenomenon is demonstrated in figure 17.

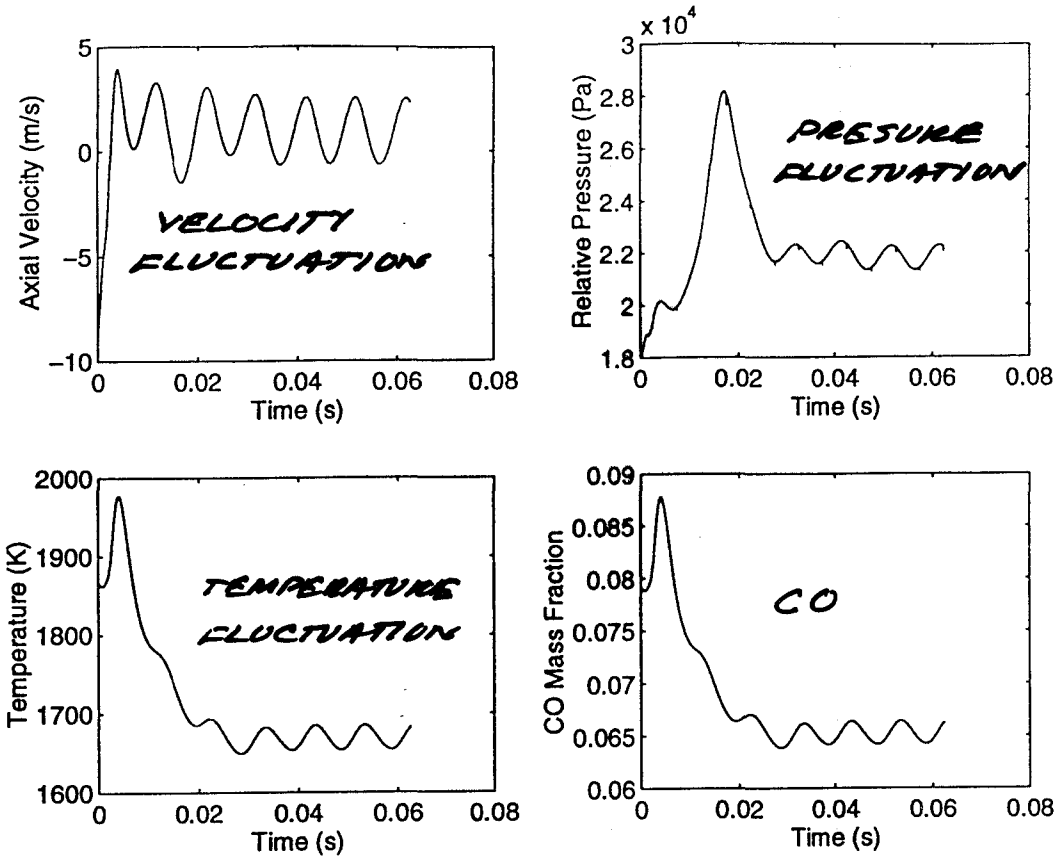


Figure 10 - Time History Curves of U, P, T, CO at Point B: Center of Diffusion Flame

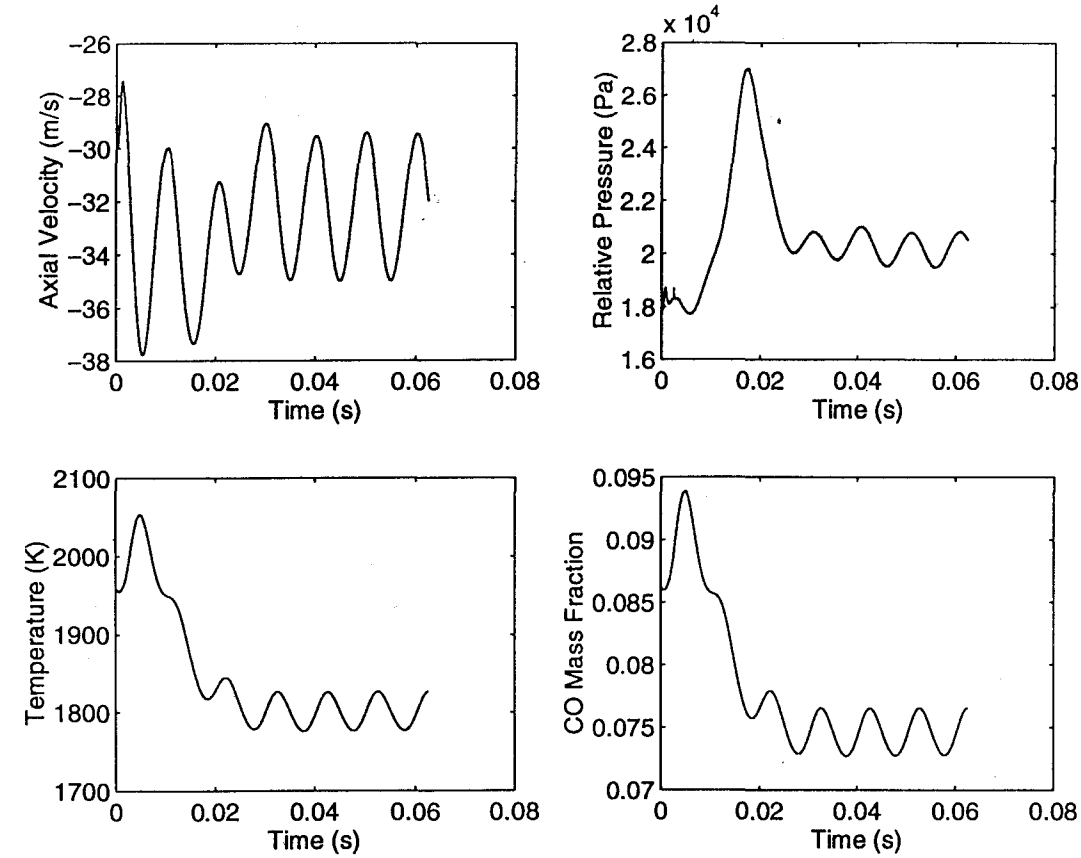


Figure 11 - Time History Curves of U, P, T, CO at Point E: Center of Recirculation Zone

Figure 3: Concentration Variation with Temperature

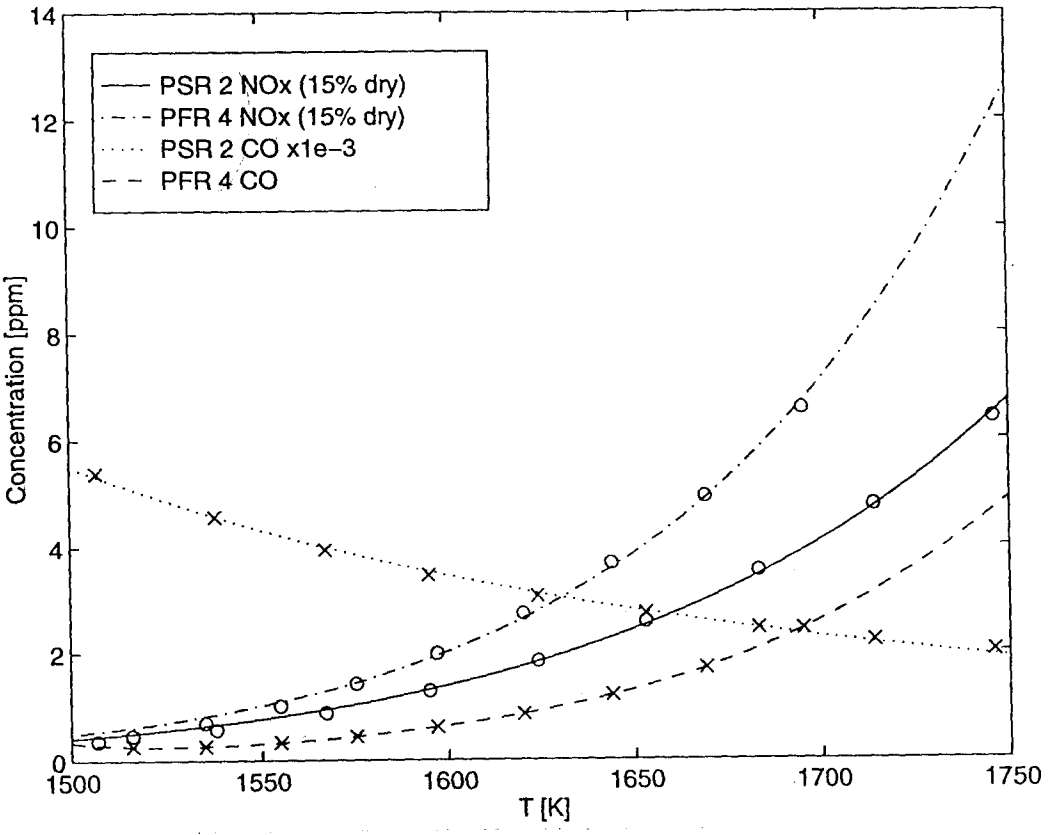


Figure 4: Temperature Oscillation for PSR 2

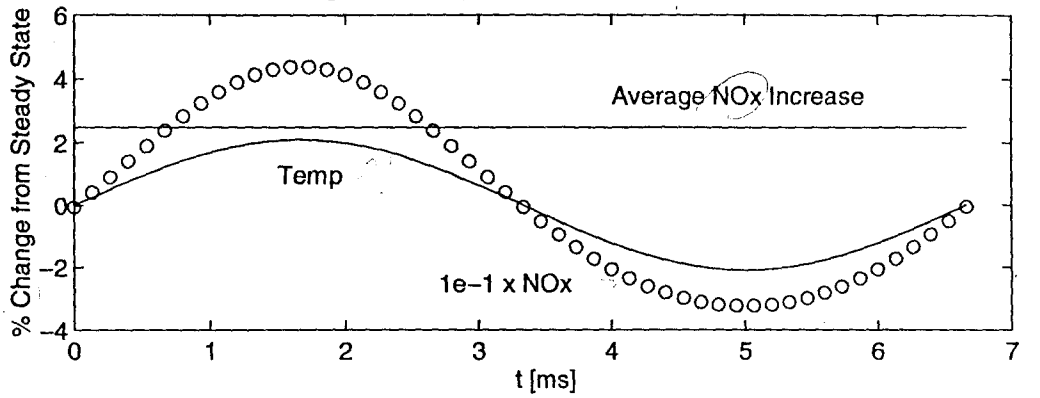


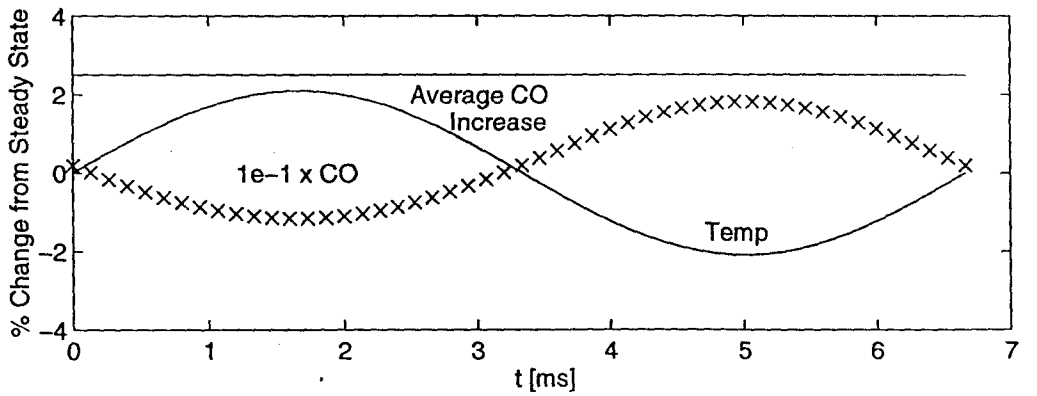


PRODUCTS: FORMULATION WITH PSRs & PFRs

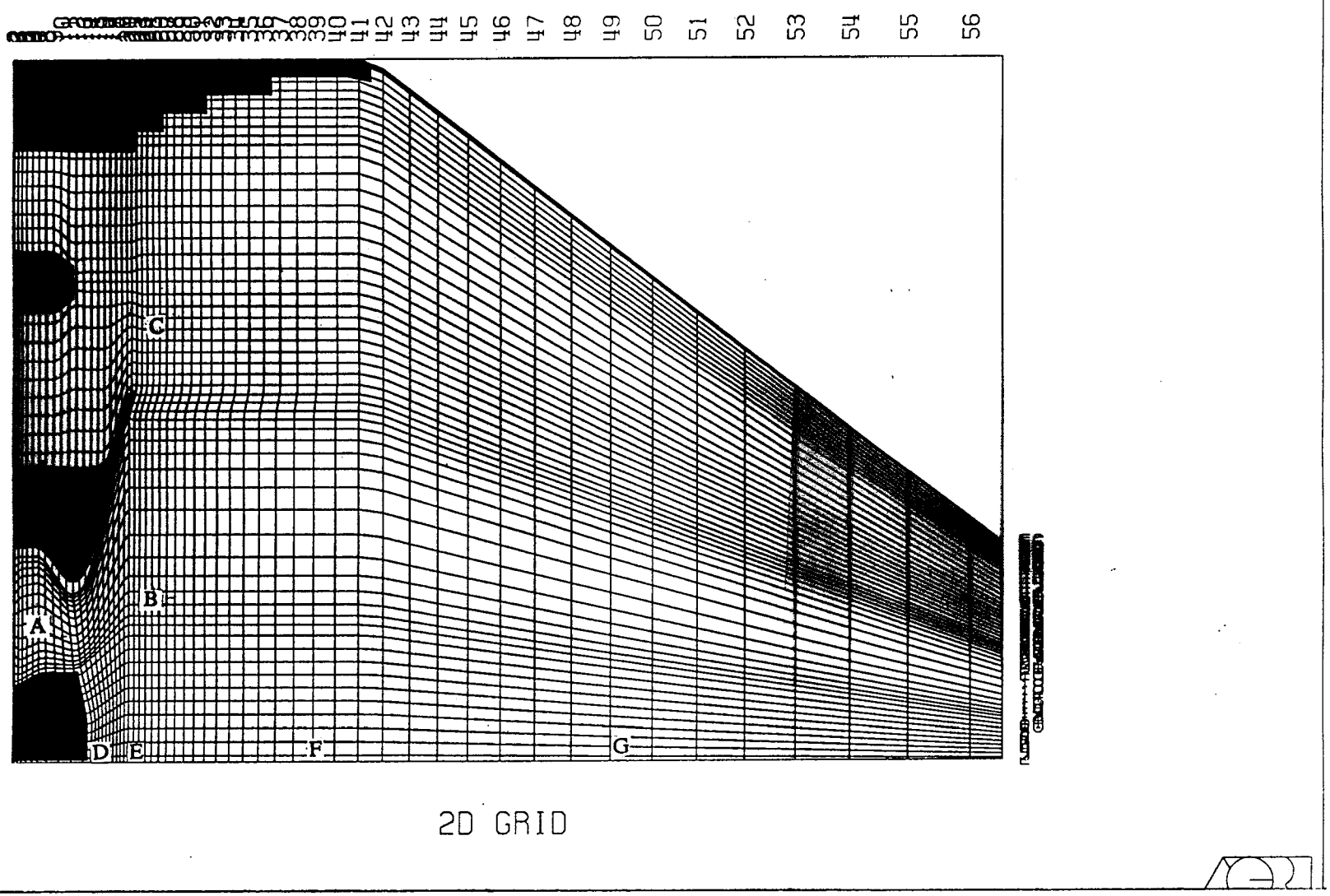


Figure 6 - 2D Grid Used for Numerical Simulations; Letters Denote Transient History Recording Points

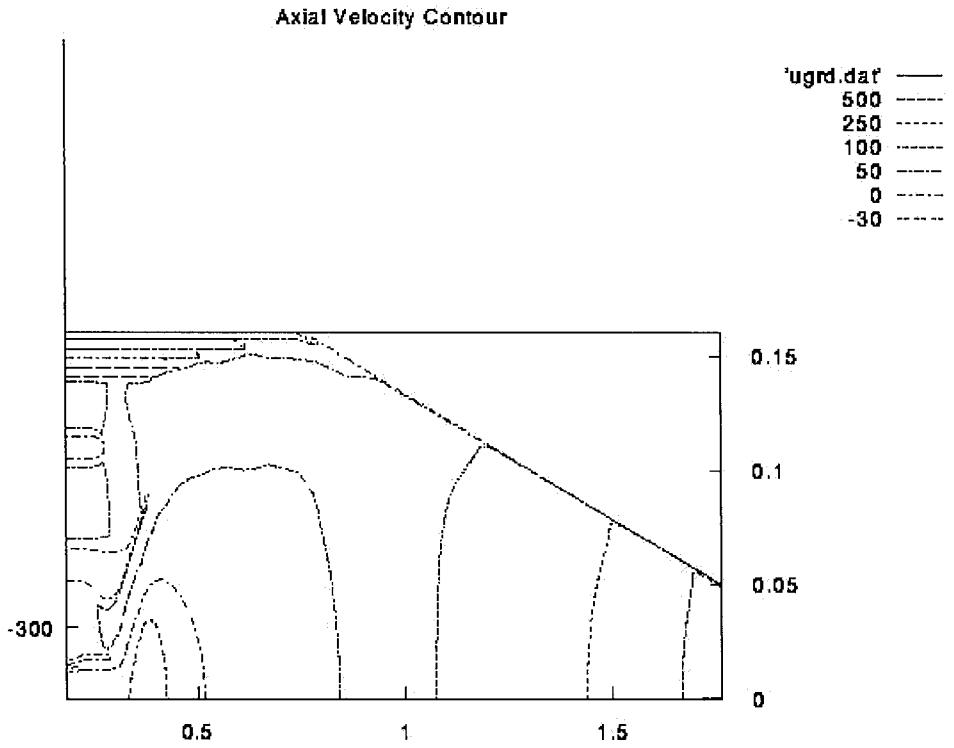


Figure 8 - Steady State Axial Velocity Contour for Gas-Turbine Combustor

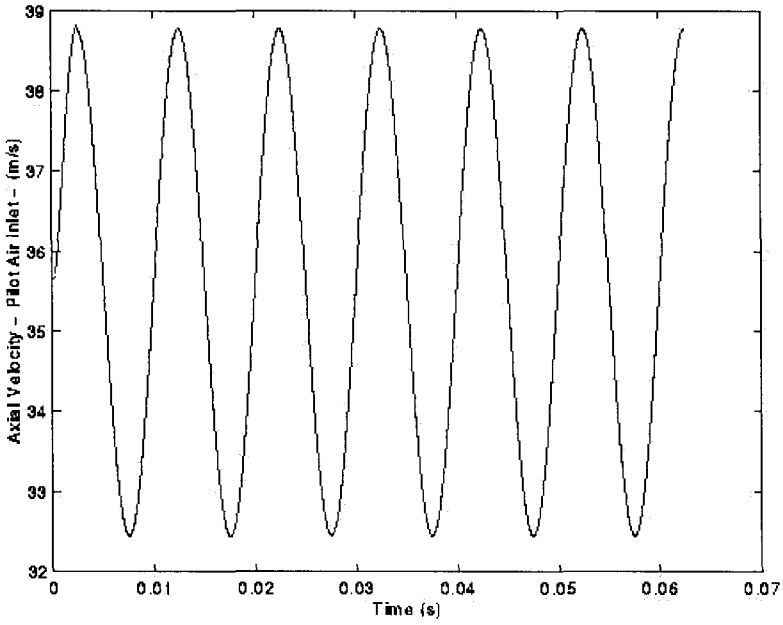


Figure 9 - Imposed Oscillating Axial Velocity versus Time at Point A: the Pilot Air Inlet

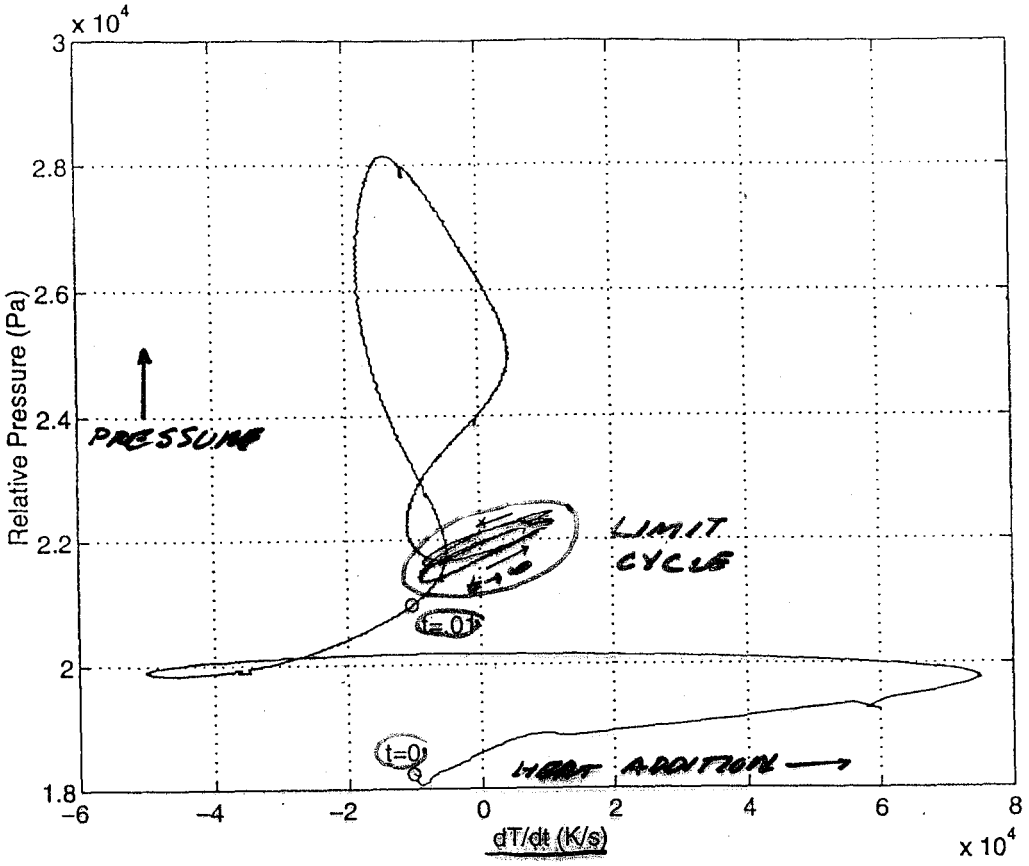


Figure 14 - Phase Plots of Pressure versus Time Derivative of Temperature at Point B

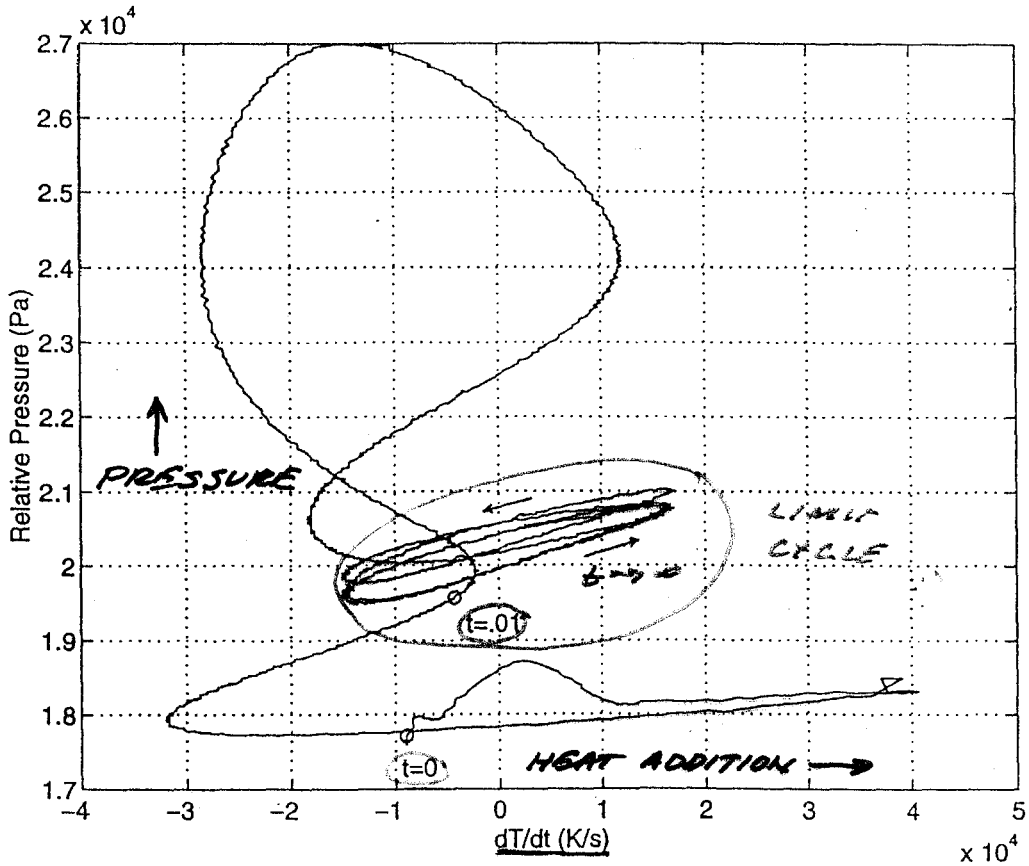


Figure 15 - Phase Plots of Pressure versus Time Derivative of Temperature at Point E

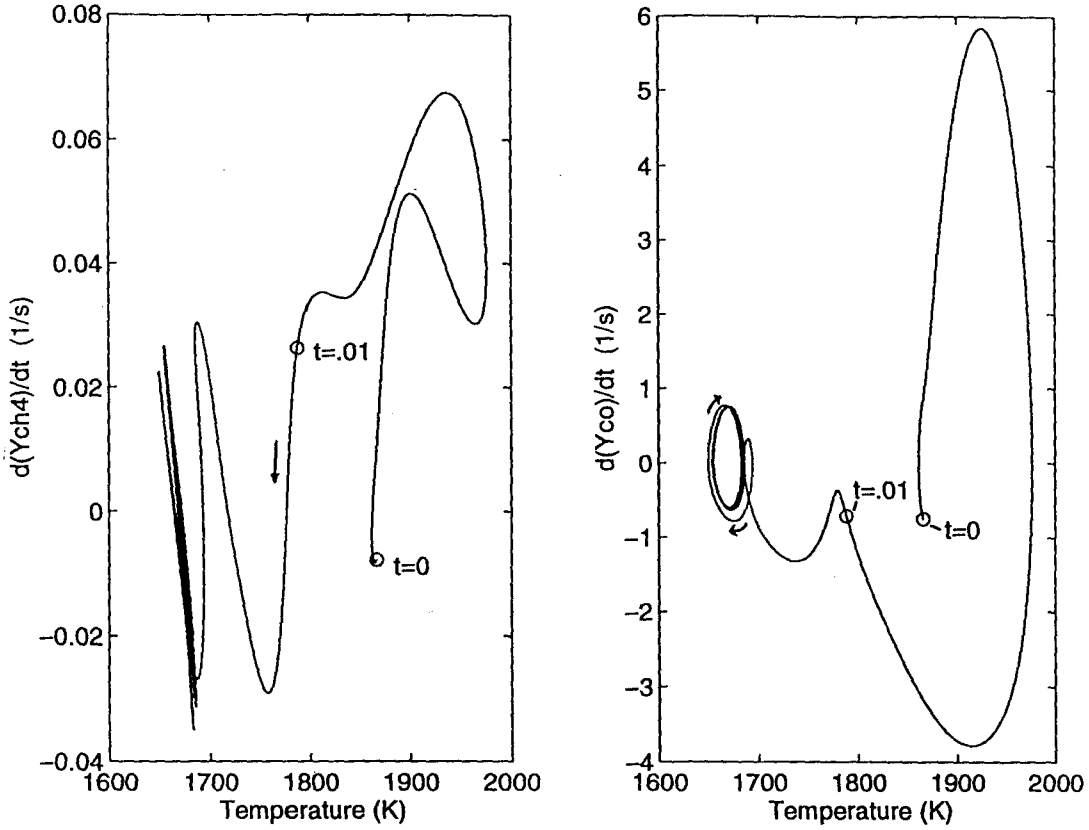


Figure 16 - Phase Plots of Time Derivative of $CH_4$ and CO versus Temperature at Point B

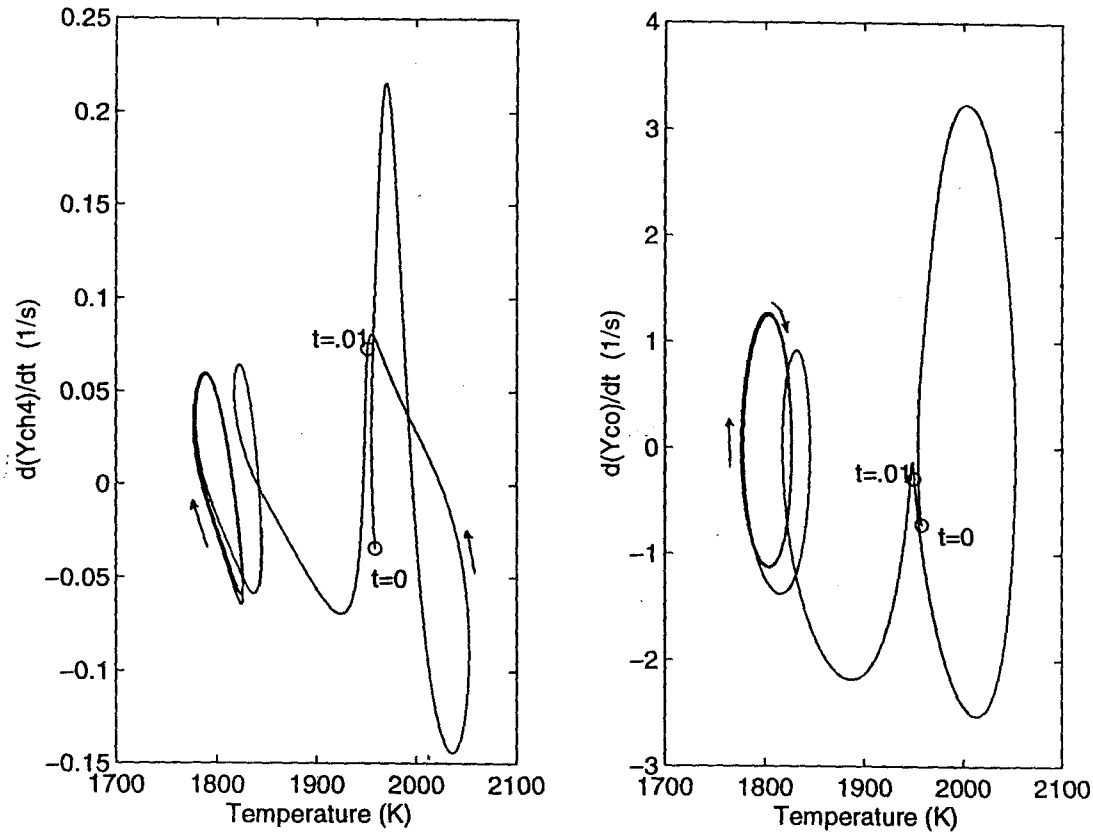


Figure 17 - Phase Plots of Time Derivative of $CH_4$ and CO versus Temperature at Point E

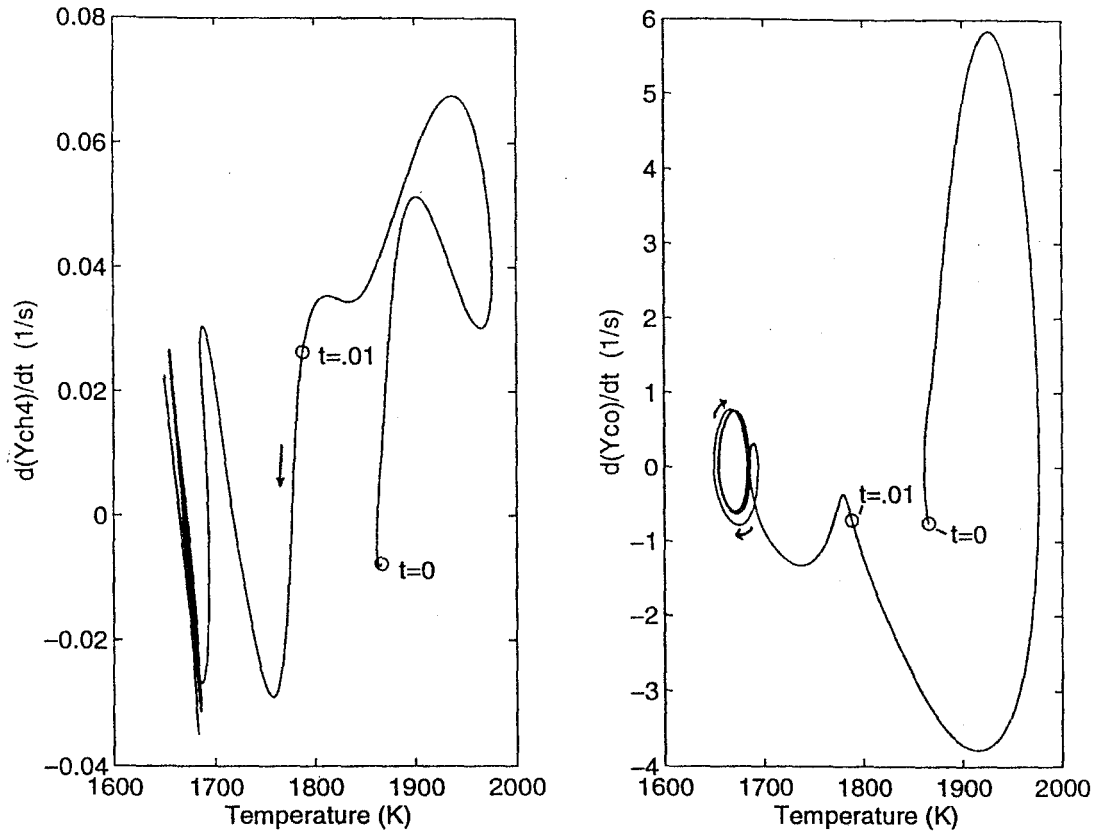


Figure 16 - Phase Plots of Time Derivative of $CH_4$ and CO versus Temperature at Point B

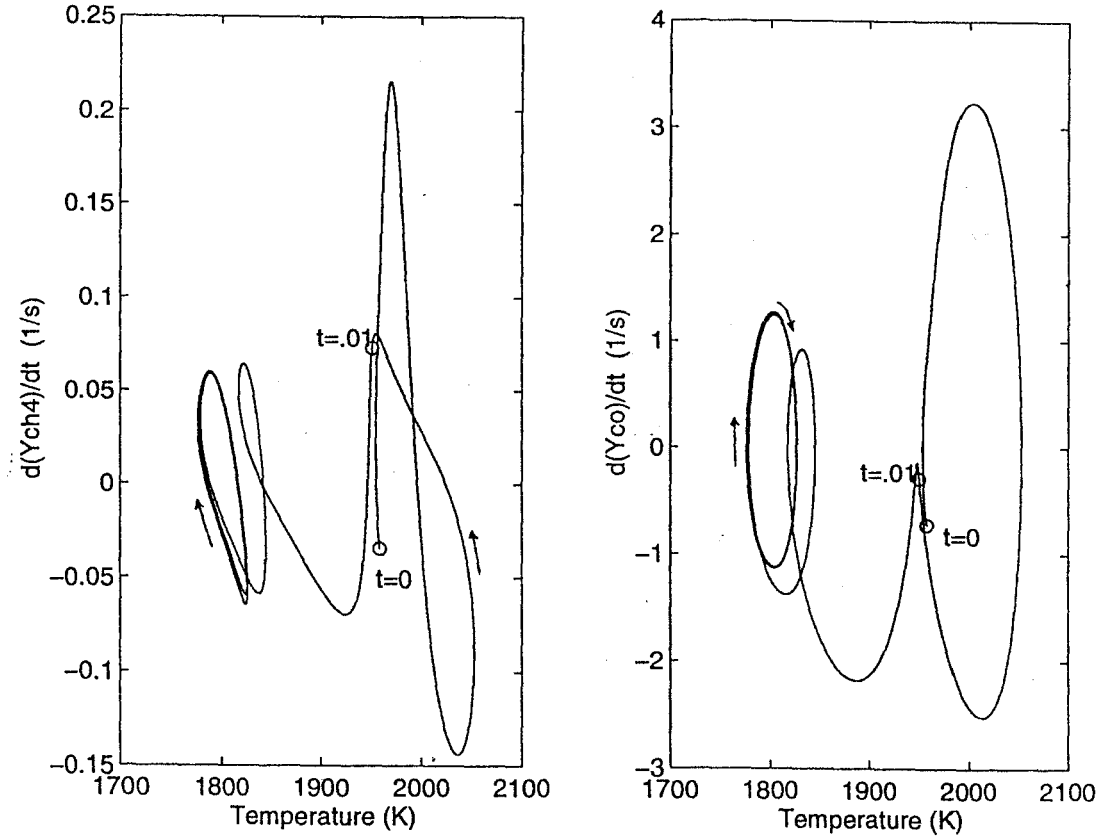


Figure 17 - Phase Plots of Time Derivative of $CH_4$ and CO versus Temperature at Point E

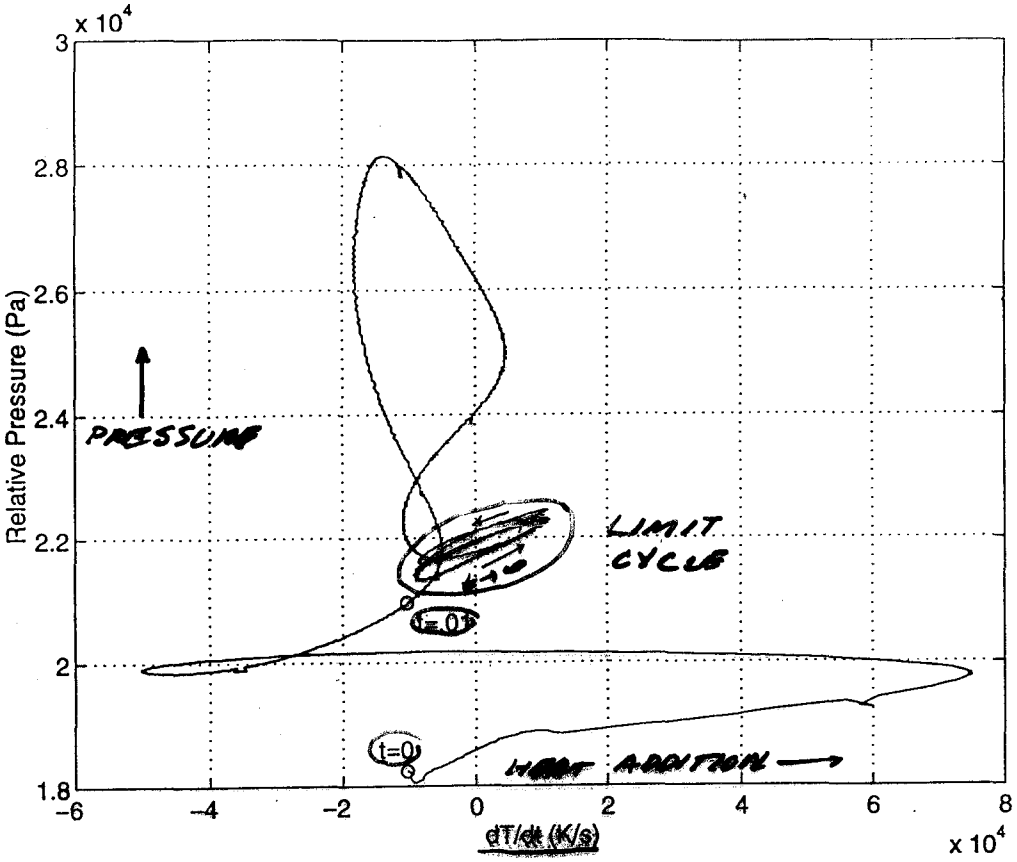


Figure 14 - Phase Plots of Pressure versus Time Derivative of Temperature at Point B

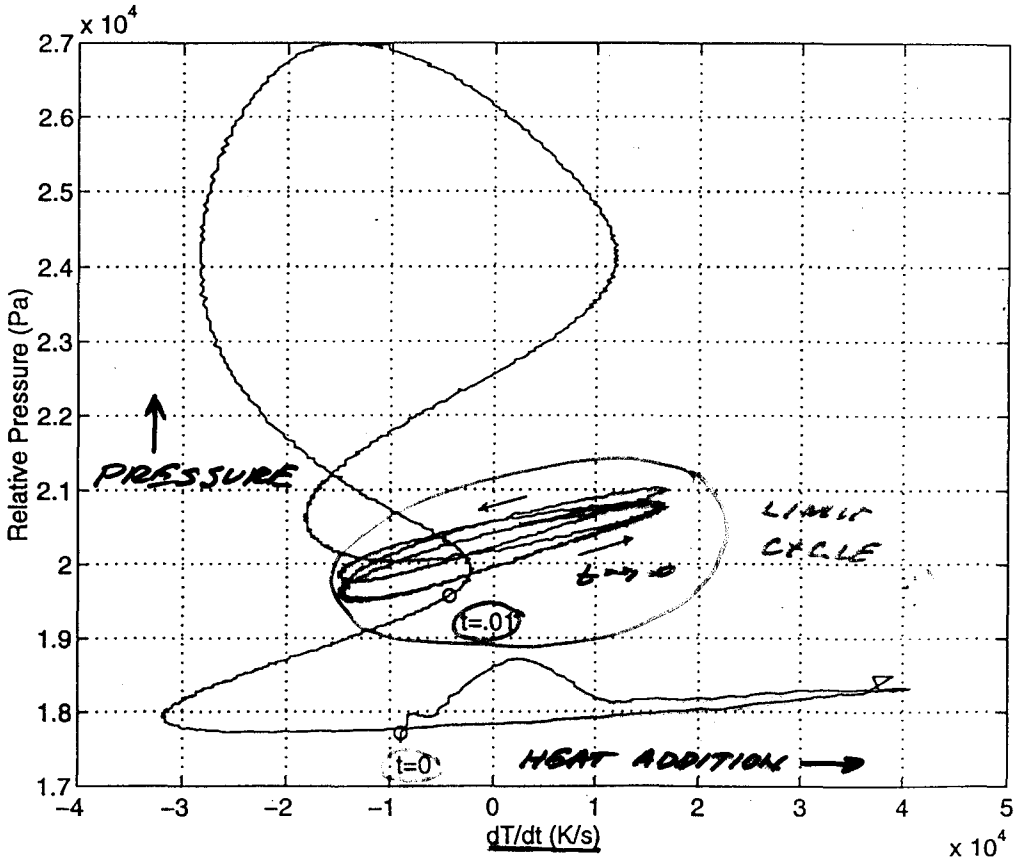


Figure 15 - Phase Plots of Pressure versus Time Derivative of Temperature at Point E

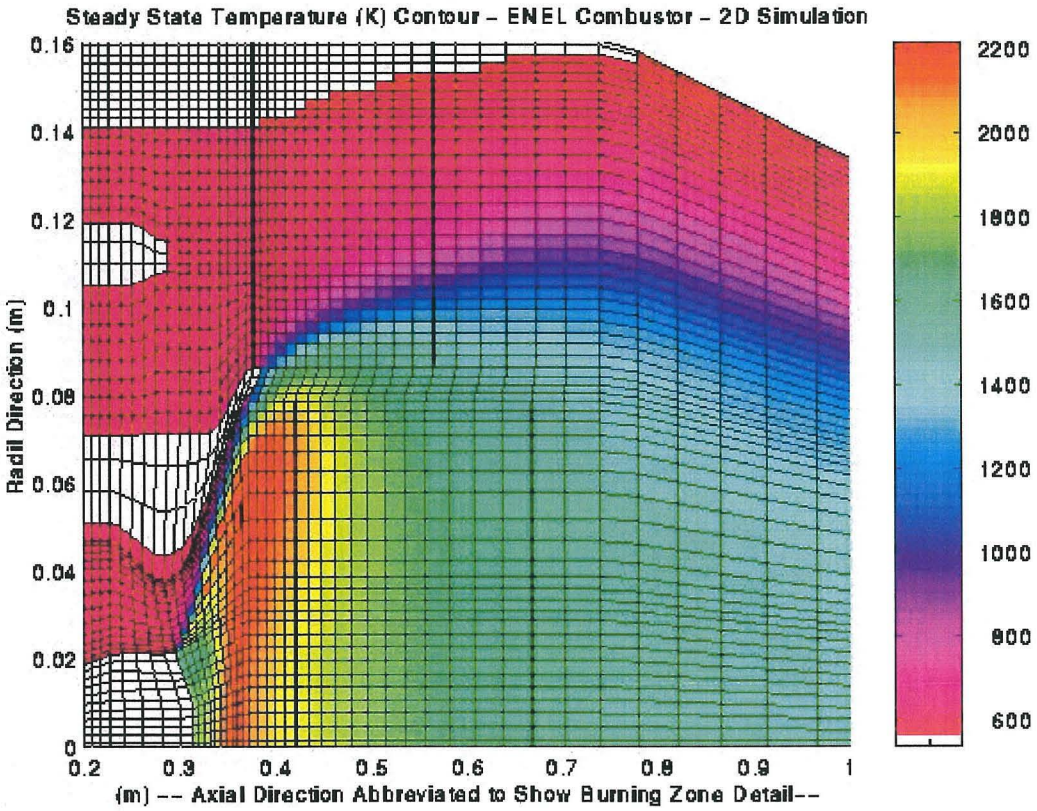


on Grants zip disk

SSTMP2D.jpg

7

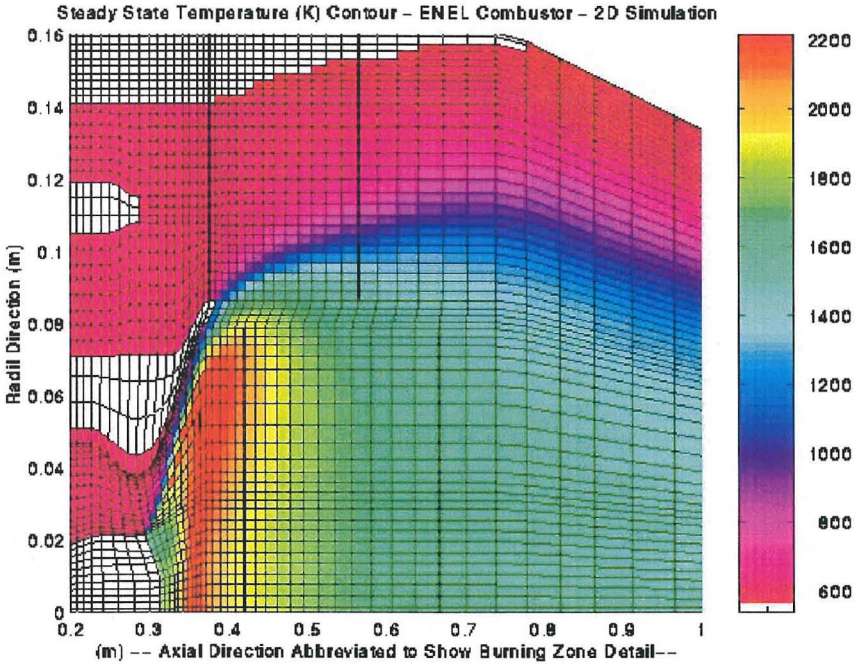
Steady State Temperature (K) Contour – ENEL Combustor – 2D Simulation
Radil Direction (m)
0.16
0.14
0.12
0.1
0.08
0.06
0.04
0.02
0
0.2
0.3
0.4
0.5
0.6
0.7
0.8
0.9
1
(m) -- Axial Direction Abbreviated to Show Burning Zone Detail--
2200
2000
1800
1600
1400
1200
1000
800
600